Measuring precise fusion cross sections using an 8T superconducting solenoid

L. T. Bezzina[1,*], E. C. Simpson[1], D. J. Hinde[1], M. Dasgupta[1], I. P. Carter[1], and D. C. Rafferty[1]

[1]Department of Nuclear Physics, Research School of Physics, The Australian National University, ACT 2601, Australia

Abstract. A novel fusion-evaporation residue separator based on a gas-filled superconducting solenoid has been developed at the Australian National University. Though the transmission efficiency of the solenoid is very high, precision cross sections measurements require this efficiency to be accurately known and vitally, requires knowledge of the angular distribution of the evaporation residues. We have developed a method to deduce the angular distribution of the evaporation residues from the laboratory-frame velocity distribution of the evaporation residues transmitted by the solenoid. The method will be discussed, focusing on benchmarking examples for ^{34}S+^{89}Y, where the angular distributions have been independently measured using a velocity filter (A. Mukherjee *et al.*, Phys. Rev. C. **66**, 034607 (2002)) . The establishment of this method now allows the novel solenoidal separator to be used to obtain reliable, precise fusion cross-sections.

1 Introduction

Heavy-ion fusion is a complex, many-body quantum process, whereby two separate nuclei merge to form a single, compact compound nucleus. It is intrinsically dissipative, requiring the kinetic energy of the collision to be dispersed into a multitude of internal nucleonic excitations. Existing models of fusion, accounting for the coherent superposition of collective excited states [2], have been quite successful in predicting the outcome of fusion at energies near and below the fusion barrier. Crucially, however, these models do not explicitly treat the progression of the system from a fully coherent quantum state to the thermalised, compact compound nucleus. As a consequence, predictions of fusion cross sections at above barrier energies with these models may disagree with experiment by up to a factor of 2 [3].

Determining the variables which control this thermalisation is a key step in understanding the progression towards a fully energy-dissipated compound nucleus. One variable thought to be important is the amount of nuclear matter overlap at the barrier radius. This matter overlap is controlled by the entrance channel charge product, Z_pZ_t [2], where Z_p is the proton number of the projectile, and Z_t is the proton number of the target. By forming the same compound nucleus (our fused product) with four different projectile-target combinations and examining the fusion cross section as a function of Z_pZ_t, we aim to isolate the nuclear matter overlap at the barrier [3].

In order to measure the total fusion cross section, it will be necessary to measure both outcomes of compound nucleus formation, namely: fusion-fission and emission of nucleons or clusters of nucleons to form an evaporation residue (ER). Due to conservation of momentum, the evaporation residue angular distribution is forward focused, which means that the measurement of evaporation residues presents a significant challenge: how to separate the large elastically scattered background from the desired evaporation residues? At the ANU, this separation is carried out using the SOLITAIRE device [4], a gas-filled separator based around an 8 T superconducting solenoid.

2 SOLITAIRE

The superconducting solenoid for in-beam transport and identification of recoiling evaporation-residues (SOLITAIRE) [4] utilises the magnetic field of the solenoid to separate evaporation residues from the intense background of elastically scattered beam. The solenoid's bore is filled with low-pressure helium gas, which brings the evaporation residues to an equilibrium charge state distribution dependent on their velocity [5]. As the scattered beam particles have a higher velocity than the evaporation residues, they have higher charge states. The solenoid's magnetic field effectively acts as a thin lens, with a focal length characterised by [6]:

$$f \approx \frac{4p^2}{q^2 B_z L}, \tag{1}$$

where p and q are the momentum and ionic charge state of the particle entering the solenoid, B_z is the z-component of the solenoid's magnetic field, and L is the length of the solenoid. Thus the magnetic field of the solenoid can be set to focus the evaporation residues onto SOLITAIRE's two multi-wire proportional counters (MWPCs), while the elastically scattered beam particles are intercepted on an axial blocking rod and discs before the MWPCs, preventing them from exiting the solenoid. Figure 1 is a schematic

*e-mail: lauren.bezzina@anu.edu.au

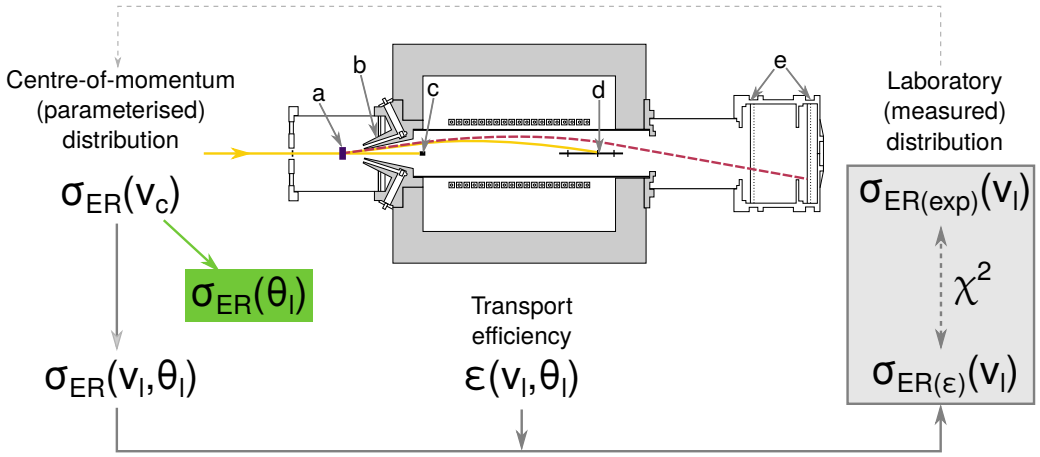

Figure 1. Flowchart of the method for extracting precise angular distributions from measurements made with the SOLITAIRE device, with a schematic of the device and labels of its key features included for context. The labelled components are (a) the target, (b) the iron cone forming part of the solenoid's magnetic shielding (all of which is indicated by the shaded grey areas), (c) the Faraday cup, used to catch the direct beam, (d) the axial blocking rod and discs and (e) the two multi-wire proportional counters (MWPCs). Example radial trajectories are also included for an elastically scattered beam particle (orange line) and an evaporation residue (dashed pink line). The flowchart shows the routine described in Section 3, including the initialisation step for estimating initial parameters of the $\sigma_{ER}(v_c)$ distribution, and the final transformation to the angular distribution $\sigma_{ER}(\theta_l)$.

diagram of SOLITAIRE, also showing the radial coordinate of the typical paths mapped by the elastically scattered beam and evaporation residues. An elastically scattered beam trajectory is indicated by the pale orange line and an evaporation residue trajectory by the purple line. The method discussed in Section 3 is also depicted in the form of a flowchart. One of the main advantages of using SOLITAIRE is its large solid angle of acceptance (86 msr), which is the major contributor to the device's high efficiency. There are two main obstructions which define the angular acceptance, and hence reduce the overall efficiency. One is the Faraday cup immediately behind the target, which captures the direct beam, but also obstructs any evaporation residues travelling between 0 and 1°. The other is the iron cone which forms part of the solenoid's magnetic shielding, which will block any ERs at angles greater than ∼ 9°. This angular dependence is clearly seen in the efficiency profile of Fig. 2. With this angular dependence of the efficiency, it is vital to know the angular distribution of the ERs. To precisely know the angular distribution of the ERs, the measured distribution must be corrected for the transport efficiency of the device. That is, the probability of an ER exiting the target at a particular velocity and angle reaching SOLITAIRE's MWPCs after the solenoid exit. By performing Monte-Carlo simulations of the transport efficiency for a particular velocity and angle, it is possible to design an iterative correction procedure to deduce both the corrected angular distribution and total transmission efficiency of the device. The procedure and its constituent components will be described in the next section.

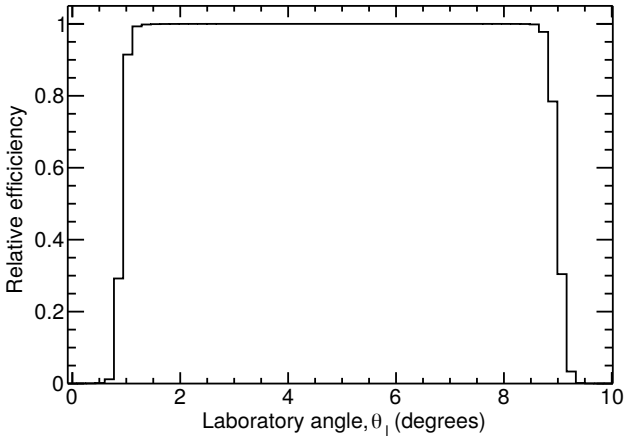

Figure 2. The transport efficiency of SOLITAIRE as a function of laboratory angle demonstrating the high efficiency for particles that are not stopped from entering the solenoid.

3 Method

As the MWPCs are position-sensitive, one may hope to use the measured radial distribution of ERs to directly reconstruct the angular distribution at the exit of the target. Previous work found, however, that this approach is very sensitive to angular scattering in the He gas, which spreads the trajectories of the ERs and requires detailed phenomenological modelling to accurately reconstruct the angular distribution [7]. A new and more reliable approach has therefore been conceived, using the velocity distribution of the ERs, easily deduced from the pulsed beam and timing signals from the MWPC centre-foil.

The laboratory-frame velocity and angular distributions are linked through the centre-of-momentum velocity distribution, denoted $\sigma_{ER}(v_c)$. As outlined by Weisskopf [8], the distribution of ER velocities in this frame is expected to take the shape of one of more Maxwellian distributions. This expectation arises from the statistical

treatment of the compound nucleus (CN), justified due to the high level-density of states accessible to the constituent nucleons. Single neutron evaporation then results in ERs with a Maxwellian distribution of velocities. Charged-particle evaporation would result in Maxwellian distributions offset from zero due to the Coulomb repulsion between the emitted particle and remaining residue. For each residue, it is likely that a series of emissions will have occurred.

These factors lead us to parameterise $\sigma_{ER}(v_c)$ using the sum of two Maxwellians, the first representing proton and neutron emission (pxn and xn), and the second describing αxn emission. The initialising step of this procedure is to use the measured laboratory-frame velocity distribution to construct a centre-of-momentum frame distribution (using a method described in [7]), and fit this distribution with the parameterised form.

Next, the parameterised distribution is used to construct a two-dimensional distribution in laboratory velocity and angle, $\sigma_{ER}(v_l, \theta_l)$. This two-dimensional distribution is then filtered by the solenoid's transport efficiency as a function of the same parameters, $\varepsilon_T(v_l, \theta_l)$, where $\varepsilon_T(v_l, \theta_l)$ is determined from Monte Carlo simulations. Following this filtering, the two-dimensional distribution is projected onto the velocity axis, resulting in a velocity distribution filtered by the efficiency, $\sigma_{ER(\varepsilon)}(v_l)$. This theoretical distribution is compared to the measured distribution, $\sigma_{ER(exp)}(v_l)$ by computing the χ^2 between the two. This series of transformations [beginning with the construction of the two-dimensional distribution $\sigma_{ER}(v_l, \theta_l)$] is then repeated with variations in the parameters of the Maxwellians until the χ^2 between the two distributions is minimised. Once this is achieved, it can be expected that the centre-of-momentum distribution $\sigma_{ER}(v_c)$ is representative of the distribution of ERs leaving the target, unaffected by the solenoid's transport efficiency, and so can be used to construct the laboratory-frame angular distribution of ERs, $\sigma_{ER}(\theta_l)$. The entire routine is presented as a flow chart in Fig. 1.

4 Results

An example of the final, optimised laboratory velocity distribution is shown along with the experimentally measured distribution in Fig. 3 for the benchmark reaction of E_{beam} = 112 MeV ^{34}S+^{89}Y, measured with the 6.5 T version of SOLITAIRE. It is clear that the relative magnitude of the components and the shape of the distributions are in good agreement.

The deduced angular distribution for the same reaction is then compared to an independent experimental measurement in the top part of Fig. 4, where excellent agreement is seen between the two distributions. The two-shouldered structure results from the distinct contributions of proton and neutron evaporation, most significant for the more forward angles, and αxn evaporation, which defines the shoulder at $\sim 8°$. The agreement is particularly remarkable when considering the time taken for the acquisition of both data sets: the velocity distribution takes only tens

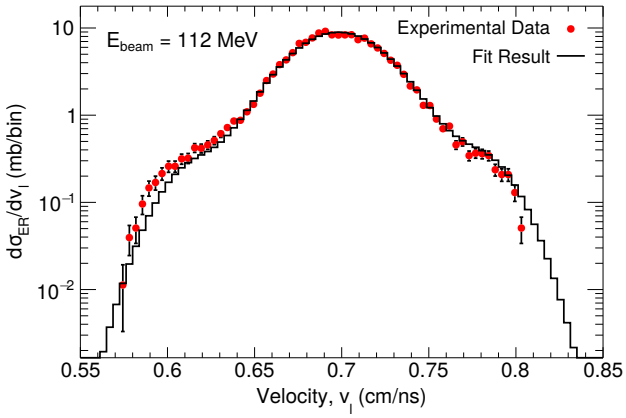

Figure 3. The laboratory-frame velocity distribution at E_{beam} = 112 MeV, where the experimental data are shown as red points, and the result of the correction routine is shown as a black histogram. Both the experimental and fitted distributions are filtered by the SOLITAIRE transmission efficiency.

of minutes to acquire, while the angle-by-angle measurement made with a velocity filter takes up to a day to acquire enough statistics for each angle.

The integrated transport efficiency of the device can be found by comparing the two-dimensional cross section $\sigma_{ER}(v_l, \theta_l)$ before and after filtering by $\varepsilon(v_l, \theta_l)$. For the E_{beam} = 112 MeV case, the integrated efficiency is 93%.

Discrepancies still exist for another benchmarking measurement of the same system at a different beam energy (E_{beam} = 124 MeV), as seen in the bottom half of Fig. 4. Here, the cross section is significantly underestimated at forward angles, and no amount of renormalisation can modify the shape of the distribution in order to bring it into agreement with the independently measured distribution. We suggest that this disagreement has its origins in the chosen form of the centre-of-momentum velocity distribution. Currently both systems are fit using the sum of two Maxwellians: one representing residues resulting from evaporation of protons and neutrons, the other representing αxn evaporation. At the lower beam energy, where proton evaporation is expected to be less likely, it appears these two Maxwellians are sufficient to describe the angular distribution of ERs. At the higher beam energy, however, it is possible the system is better described by the sum of three Maxwellians, one each for xn, pxn and αxn emission. Indeed, attempts were made to fit the measured velocity distribution with the parameterised form of $\sigma_{ER}(v_c)$ composed of the sum of three Maxwellians, but there are insufficient counts in the measured data to fully constrain the parameters, and further measurements are needed to investigate this possibility.

5 Conclusions and Future Work

A new method to extract precise ER cross sections and quantify the transmission efficiency of the SOLITAIRE separator has been developed. The routine, based on an iterative correction procedure, has been benchmarked

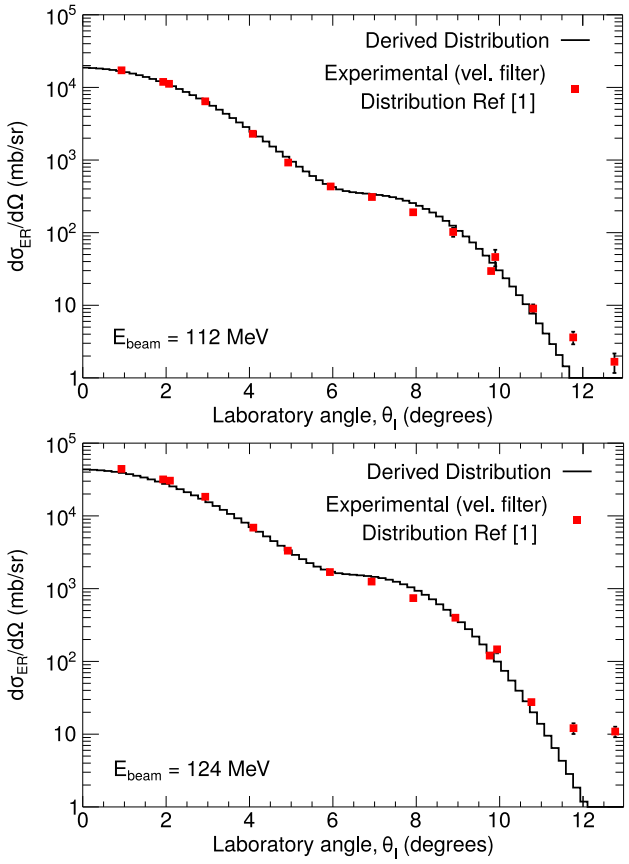

Figure 4. The differential cross section $d\sigma_{ER}/d\Omega$ as a function of laboratory angle, θ_l, for E_{beam} = 112 MeV (top) and E_{beam} = 124 MeV (bottom). The results of the minimisation routine are shown as black histograms, while independent experimental data [1] are shown by red squares.

against the reaction of ^{34}S+^{89}Y at two beam energies: 112 MeV and 124 MeV. The integrated transport efficiency of the device has been quantified at 93% for the lower energy case, and 86% for the higher energy case. Good agreement has been found between the deduced angular distributions and independently measured angular distributions for the same reaction. However more significant disagreement for the higher energy case suggests further investigation into the chosen form of the ER recoil distribution $\sigma_{ER}(v_c)$ is necessary. This exploration will be undertaken with the new 8 T version of SOLITAIRE, using the ^{28}Si+^{144}Sm reaction, for which independent angular distribution measurements are also available.

References

[1] A. Mukherjee, M. Dasgupta, D. J. Hinde, *et al.*, Phys. Rev. C. **66**, 034607 (2002).
[2] M. Dasgupta, D. J. Hinde, N. Rowley, *et al.*, Annu. Rev. Nucl. Part. S. **48**, 401 (1998).
[3] J. O. Newton, R. D. Butt, M. Dasgupta, *et al.*, Phys. Rev. C **70**, 024605 (2004).
[4] M. D. Rodríguez, M. L. Brown, M. Dasgupta, *et al.*, Nucl. Instrum. Meth. A **614**, 119 (2010).
[5] H. D. Betz, Rev. Mod. Phys. **44**, 465 (1972).
[6] O. Klemperer, M. E. Barnett, *Electron Optics* (Cambridge University Press, 1953), ISBN: 9780521179737.
[7] I. P. Carter, M. L. Brown, M. Dasgupta, *et al.*, EPJ Web. Conf. **35**, 05003 (2012).
[8] V. Weisskopf, Phys. Rev. **52**, 295 (1937).